Polarizabilities of the beryllium clock transition

J. Mitroy*
School of Engineering, Charles Darwin University, Darwin NT 0909, Australia
(Received 19 September 2010; published 22 November 2010)

The polarizabilities of the three lowest states of the beryllium atom are determined from a large basis configuration interaction calculation. The polarizabilities of the $2s^2\ ^1S^e$ ground state ($37.73a_0^3$) and the $2s2p\ ^3P_0^o$ metastable state ($39.04a_0^3$) are found to be very similar in size and magnitude. This leads to an anomalously small blackbody radiation shift at 300 K of $-0.018(4)$ Hz for the $2s^2\ ^1S^e$–$2s2p\ ^3P_0^o$ clock transition. Magic wavelengths for simultaneous trapping of the ground and metastable states are also computed.

DOI: 10.1103/PhysRevA.82.052516 PACS number(s): 32.10.Dk, 31.15.V−, 31.15.ap, 32.70.Cs

I. INTRODUCTION

The present article reports the polarizabilities that govern the response of the neutral beryllium atom to an applied electric field. One of the primary reasons for the present work is the recent developments in the field of ultracold atom physics [1–3]. One area of particular interest is the development of optical lattice clocks [4–6]. One of the major impediments to the development of optical frequency standards achieving 10^{-18} relative precision is the shift of the atomic levels due to the ambient fields of the apparatus in which the clock atoms are located, i.e., the blackbody radiation (BBR) shift [7]. The two states in the beryllium $2s^2\ ^1S^e$–$2s2p\ ^3P^o$ clock transition have almost the same polarizabilities, leading to a BBR shift that is more than two orders of magnitude smaller than the BBR shift of the clock transition in strontium [8].

There have been some previous investigations of the beryllium polarizabilities [9–21]. These have mainly focused on the ground state and only a few calculations have been performed for any of the excited states [10,14,19].

In the present study, the static polarizabilities of the three lowest states of beryllium are computed. The dynamic polarizability is also determined and the magic wavelengths for the simultaneous trapping of the $2s^2\ ^1S^e$ ground state and the $2s2p\ ^3P_0^o$ excited state are determined.

II. METHODOLOGY OF CALCULATION

A. The CI calculations of the Be states

The CI calculations used to generate the physical and L^2 pseudostates were very similar to those used previously to determine the dispersion interaction parameters of the Be ground state and the metastable $^3P^o$ state [9,10,22]. One difference between the present calculation and the earlier calculations [9,10,22] is that the present orbital basis is larger.

There were a total of 152 valence orbitals with a maximum orbital angular momentum of $\ell = 5$. The radial dependence of the orbitals was described by a mixture of Slater-type orbitals (STOs) and Laguerre-type orbitals (LTOs) [9,22]. The number of active orbitals for $\ell = 0 \rightarrow 5$ were 27, 30, 30, 25, 20, and 20, respectively. The wave function for the $1s^2$ core was taken from a Be^{2+} ground-state Hartree-Fock (HF) wave function computed by a program written by the present author [23] using a $(4s)$ STO basis. The exponent set was generated using a nonlinear optimization. Some $\ell = 0$ valence orbitals were generated from the STOs used for the core. All the other orbitals were written as LTOs due to the superior linear dependence properties of LTOs when compared with STO basis sets. The use of the large orbital basis resulted in wave functions and energies for the low-lying states that were close to convergence. The length of the CI expansions for the different states ranged from 1500 to 4500.

The effective Hamiltonian for the two valence electrons was essentially a fixed core Hamiltonian with the addition of semi-empirical potentials to allow for the polarization interaction with the core [9,11]. The direct and exchange interactions of the valence electrons with the HF wave function used to represent the core were calculated exactly. The semi-empirical core polarization potential has a dipole polarizability of $\alpha_d = 0.0523a_0^3$ [9,24]. This potential included both one-body and two-body terms [9,24]. The cutoff parameters of the polarization potential were fixed by tuning the low-lying states of Be^+ to the experimental energies. They were $\rho_0 = 0.941a_0$, $\rho_1 = 0.895a_0$, and $\rho_2 = 1.20a_0$ [24]. The cutoff parameter for the two-body potential was set to the s-wave value of $0.941a_0$. Some additional small adjustments to the cutoff parameters were made for some symmetries by tuning the Be binding energies to the experiment.

The oscillator strengths (and other multipole expectation values) were computed with operators that included polarization corrections [9,25–27]. The value of the cutoff parameter for the transition operators was $0.941a_0$. The present CI+ core polarization calculations will be referred to as the CICP calculation.

III. RESULTS

A. Energy levels

The ability of the present semi-empirical CI calculation to reproduce the low-lying spectrum can be assessed from Table I. The experimental two-electron binding energy was determined using ionization energies for Be and Be^+ [28]. The largest discrepancy between theory and experiment was about 3×10^{-4} hartrees. In a few cases, some further tunings of the polarization potential cutoff parameters were performed for individual symmetries to ensure that the energies of the neutral Be states agreed with experiment to better than

*jxm107@rsphysse.anu.edu.au

TABLE I. Theoretical and experimental energy levels (in hartrees) of the low-lying states of the Be atom. The energies are given relative to the energy of the Be^{2+} core. The experimental energies (taken from Ref. [28]) for the triplet states are averages with the usual $(2J+1)$ weighting factors.

State	Theory	Experiment
$2s^2\ ^1S^e$	−1.011 897	−1.011 851
$2s2p\ ^1P^o$	−0.817 890	−0.817 908
$2s3s\ ^1S^e$	−0.762 673	−0.762 723
$2p^2\ ^1D^e$	−0.752 636	−0.752 675
$2s3p\ ^1P^o$	−0.737 643	−0.737 617
$2s3d\ ^1D^e$	−0.718 241	−0.718 293
$2s2p\ ^3P^o$	−0.911 666	−0.911 702
$2s3s\ ^3S^e$	−0.774 467	−0.774 552
$2s3p\ ^3P^o$	−0.743 379	−0.743 448
$2p^2\ ^3P^e$	−0.739 865	−0.739 858
$2s3d\ ^3D^e$	−0.729 050	−0.729 113

10^{-4} hartrees. The energies tabulated in Table I are those after the final tunings.

B. Oscillator strengths

A good integrity test of the CI calculations comes from the tabulation of oscillator strengths in Table II. The notation $f_{in}^{(k)}$ is used to denote the kth multipole absorption oscillator strength from state i to state n according to the definitions given in Refs. [35,36]. The definition is

$$f_{in}^{(k)} = \frac{2|\langle\psi_i; L_i \parallel r^k \mathbf{C}^k(\hat{\mathbf{r}}) \parallel \psi_n; L_n\rangle|^2 \epsilon_{ni}}{(2k+1)(2L_i+1)}. \qquad (1)$$

In this expression, $\epsilon_{ni} = (E_n - E_i)$ is the energy difference between the initial state and final state, L_i and L_n are the orbital angular momenta of states i and n, k is the multipolarity of the transition, and $\mathbf{C}^k(\hat{\mathbf{r}})$ is a spherical tensor.

Besides the present calculation, data from three other calculations are included. These are the time-dependent gauge invariant (TDGI) calculations of Refs. [14,19], the B-spline CI calculation of Chen [30] with a semi-empirical core potential (BCICP), and finally, the B-spline CI calculations (BCIBP) using a Briet-Pauli Hamiltonian by Froese-Fischer and Tachiev [29]. In a number of respects, the BCICP calculation is similar to the present calculation; core-valence correlations are included with a semi-empirical polarization potential and the orbital space for the valence particles was large. The biggest systematic *ab initio* calculation performed would seem to be the BCIBP [29]. This calculation allowed for core correlations, core-valence correlations, and valence correlations. All the oscillator strengths quoted from these other works are derived from transition matrix elements computed using the length form of the multipole operators.

The TDGI calculations give the least accurate oscillator strengths. The TDGI oscillator strength for the resonant $2s^2\ ^1S^e \rightarrow 2s2p\ ^1P^o$ transition is the largest. Further, their $^3D^e \rightarrow\ ^3P^o$ oscillator strengths are substantially different from any of the other calculations and also disagree with experiment. The TDGI oscillator strengths were mainly quoted to show the limitations of this method for calculating polarizabilities.

The present calculation gives $f^{(1)}_{2s^2\rightarrow 2s2p} = 1.3743$. This is compatible with the BCICP and BCIBP values. A thorough theoretical evaluation using state of the art theory recommended a value of 1.375(7) for the resonance transition [37].

There is a general degree of consistency between the present oscillator strengths and those of the BCIBP and BCICP calculations. These oscillator strengths agree to within 5% except in those cases where the oscillator strength is anomalously small (e.g., the $2s2p\ ^1P^o \rightarrow 2p^2\ ^1D^e$ transition). In most cases, the present calculations are in better agreement with the BCICP calculators. While the CICP and BCICP calculations are not *ab initio*, the simplifications made in having a fixed core mean they represent close to exact numerical solutions of the Schrodinger equation within the confines of the underlying model potential.

C. Polarizabilities

The definitions of the scalar and tensor polarizabilities for general states have been given in Refs. [7,10] and are not repeated here. The scalar and tensor dipole polarizabilities are given in Table III. The energies of the states listed in Table I were set to their experimental values prior to evaluating the polarizability sum rules since excited-state polarizabilities can be particularly sensitive to small changes in the energy separations between different levels. The energies used for the triplet multiplets were those of the $^3P^o_0$ state and the $^3P^e_1$ and $^3D^e_1$ states. Previously, the CICP method had been used to compute polarizabilities and dispersion coefficients

TABLE II. Theoretical and experimental values of the oscillator strengths for selected transitions of the Be atom. The experimental data are taken from various sources.

	Present	Other theory			
Transition	CICP	BCIBP [29]	BCICP [30]	TDGI [14,19]	Experiment
$2s^2\ ^1S^e \rightarrow 2s2p\ ^1P^o$	1.3743	1.380	1.375	1.398	1.341(50) [31], 1.40(4) [32]
$2s^2\ ^1S^e \rightarrow 2s3p\ ^1P^o$	0.008 68	0.008 99	0.009 01		
$2s2p\ ^1P^o \rightarrow 2s3s\ ^1S^e$	0.1182	0.1147	0.118	0.128	
$2s2p\ ^1P^o \rightarrow 2p^2\ ^1D^e$	5.1[−5]	1.4[−5]	7.0[−5]	0.0006	
$2s2p\ ^1P^o \rightarrow 2s3d\ ^1D^e$	0.4095	0.3962	0.410	0.194	
$2s2p\ ^3P^o \rightarrow 2s3s\ ^3S^e$	0.0821	0.0841	0.0823	0.026	0.086(2) [33], 0.089(3) [34]
$2s2p\ ^3P^o \rightarrow 2s3d\ ^3D^e$	0.2944	0.2994	0.295	0.154	0.29(1) [33], 0.29(1) [34]
$2s2p\ ^3P^o \rightarrow 2p^2\ ^3P^e$	0.4463	0.4452			

TABLE III. The static and tensor dipole polarizabilities for some low-lying states of beryllium. The quadrupole moments are also given.

	α_d (a.u.)		$\alpha_{d,2LL}$ (a.u.)		Q (a.u.)
State	Present	Other	Present	Other	Present
$2s^2\ ^1S^e$	37.73	37.755 ECG [17] 37.76 CI + MBPT [18] 37.62 TDGI [14]			
$2s2p\ ^1P^o$	121.40	130.04 TDGI [19]	−43.13	−50.30 TDGI [19]	6.15
$2s2p\ ^3P^o$	39.04	36.08 TDGI [19]	0.541	1.04 TDGI [19]	4.54

for the $2s^2\ ^1S^e$ and $2s2p\ ^3P^o$ excited states [9,10]. While the present calculation is larger, the resulting polarizabilities have undergone minimal change.

The polarizability for the $2s^2\ ^1S^e$ ground state could hardly be in any better agreement with existing high accuracy calculations. It is less than 0.05 a.u. smaller than the close to exact determination using a basis of explicitly correlated Gaussians (ECGs) [17]. Similarly, the relativistic configuration interaction plus many-body perturbation theory (CI + MBPT) values of Porsev and Derevianko [18] lie within 0.05 a.u. of the present value.

The scalar dipole polarizability for the $2s2p\ ^3P^o$ state in terms of oscillator strength sums to intermediate states, n, with $L_n = 0, 1$, and 2 given by [7,10]

$$\begin{aligned}\alpha_d &= \sum_{n,L_n=0} \frac{f_{in}^{(1)}}{\epsilon_{in}^2} + \sum_{n,L_n=1} \frac{f_{in}^{(1)}}{\epsilon_{in}^2} + \sum_{n,L_n=2} \frac{f_{in}^{(1)}}{\epsilon_{in}^2} \\ &= A_0 + A_1 + A_2, \end{aligned} \tag{2}$$

where the index i represents the $^3P^o$ state. The present calculation gives $A_0 = 5.239a_0^3$, $A_1 = 15.266a_0^3$, and $A_2 = 18.532a_0^3$, giving a scalar polarizability of $39.04a_0^3$. The TDGI $^3P^o$ polarizability is about 10% smaller than the present CICP value. The present CICP polarizability should be taken as the preferred value since the underlying description of the atomic structure in the CICP calculation is superior to that of the TDGI calculation.

The tensor polarizability for the $^3P^o$ state with $M = L = 1$ is given by [10]

$$\begin{aligned}\alpha_{d,2L_0L_0} &= -\sum_{n,L_n=0} \frac{f_{in}^{(1)}}{\epsilon_{in}^2} + \frac{1}{2}\sum_{n,L_n=1} \frac{f_{in}^{(1)}}{\epsilon_{in}^2} - \frac{1}{10}\sum_{n,L_n=2} \frac{f_{in}^{(1)}}{\epsilon_{in}^2} \\ &= -A_0 + \frac{1}{2}A_1 - \frac{1}{10}A_2. \end{aligned} \tag{3}$$

The present calculation gives $\alpha_{d,2LL} = 0.541a_0^3$. The tensor polarizability for the $J = 0$ state of this multiplet is zero. The tensor polarizability for the state with $J = 1$ is obtained from Eq. (3) by multiplying the right-hand side by $-1/2$, giving $-0.271a_0^3$. The tensor polarizability of the $J = 2$ state is $0.541a_0^3$. Table IV lists the polarizabilities of all the J, M_J states of the $^3P^o$ multiplet.

D. The $E1$ BBR shift

The electric dipole ($E1$) induced BBR energy shift of an atomic state can be approximately calculated as [18]

$$\Delta E = -\frac{2}{15}(\alpha\pi)^3\alpha_d(0)T^4(1+\eta), \tag{4}$$

where α is the fine structure constant. The static scalar polarizability $\alpha_d(0)$ and energy shift ΔE in Eq. (4) are in atomic units. In this expression, the temperature in K is multiplied by $3.166\,815\,3 \times 10^{-6}$. The BBR frequency shift (in Hz) for a given transition can be computed

$$\Delta\nu_{\rm BBR} = 6.579\,684 \times 10^{15}(\Delta E_{\rm upper} - \Delta E_{\rm lower}). \tag{5}$$

The factor η is a correction factor that allows for the frequency dependence of the polarizability when the blackbody integral is performed [8,38,39]. The factor η, referred to as the dynamic shift, is most conveniently written as [8,39]

$$\eta \approx -\frac{40\pi^2T^2}{21\alpha_d(0)}S(-4), \tag{6}$$

where $S(-4)$ is defined as

$$S(-4) = \sum_{n,L_n=0} \frac{f_{in}^{(1)}}{\epsilon_{in}^4}. \tag{7}$$

The value of $S(-4)$ for the ground state was 976.9 a.u. The scalar part of $S(-4)$ for the metastable excited state was 1174. The value of η for the ground state was 0.000 44, while the value of η for the metastable state was 0.000 51.

The BBR shift (ignoring the very small dynamic components) using the polarizabilities in Table III was 0.0112 Hz. This is more than one order of magnitude smaller than the BBR shift of any existing or proposed lattice clock [7].

All alkaline-earth lattice clocks so far in development aim to use the $^3P_0^o$ state. Another possible clock state is the $^3P_2$ state.

TABLE IV. The dipole polarizabilities for the different states of the $2s2p\ ^3P^o$ multiplet.

J	M_J	α_{J,M_J}
0	0	39.04
1	0	39.58
1	1	38.77
2	0	38.50
2	1	38.77
2	2	39.58

The dominant decay of this state is a magnetic quadrupole decay to the ground state with a transition rate of 1.70×10^{-4} s^{-1} [29]. The $M_J = 0$ magnetic sublevel of the $^3P_2$ state has a polarizability of $38.50a_0^3$ leading to an even smaller BBR shift of 0.0066 Hz.

E. The $M1$ BBR shift

The magnetic dipole components ($M1$) of the BBR field can also make a contribution to the BBR shift. One can write that $\Delta\nu_{\rm Be} = \Delta\nu_{\rm Sr}\delta E_{\rm Sr}(^3P_1^o - {}^3P_0^o)/\delta E_{\rm X}(^3P_1^o - {}^3P_0^o)$, where the $M1$ frequency shift for Sr has been estimated at 2.4×10^{-5} Hz [8]. Using $\delta E_{\rm Sr}(^3P_1^o - {}^3P_0^o) = 187$ cm^{-1} [40] and $\delta E_{\rm Be}(^3P_1^o - {}^3P_0^o) = 0.64$ cm^{-1} [41] gives -0.007 Hz, which will increase the BBR shift to -0.018 Hz.

The other possible clock state is the $^3P_2$ state. The dominant decay of this state is the magnetic quadrupole decay to the ground state [29]. In this case the dominant component to the $M1$ BBR shift comes from the $M1$ transition to the $2s2p\ ^3P_1^o$ state. The $(^3P_2^o - {}^3P_1^o)$ energy interval is 2.34 cm^{-1} [41]. In this case the $M1$ shift due to interaction with the $^3P_1^o$ state will lead to a BBR shift that tends to increase the frequency, and thus tends to partially cancel the $E1$ BBR shift.

F. The quadrupole moments

The quadrupole moment for a given J state of a multiplet is usually defined as being equal to twice the expectation value of the quadrupole operator $r^2\mathbf{C}_{20}(\mathbf{r})$ for the state with $J = M_J$. The quadrupole moments in Table I are for the states with the highest J value in each multiplet; i.e., $^1P_1^o$ and $^3P_2^o$. The quadrupole moment for the $^3P_2$ state is $4.54a_0^2$, which is effectively the same as that given by a slightly smaller CI calculation with a similar Hamiltonian [10]. No previous calculations of the $2s2p\ ^1P^o$ state quadrupole moment exist for comparison.

G. Magic wavelengths

The magic wavelength for a pair of states is the wavelength at which both states have the same ac Stark shift. This can be used for optical cooling and trapping of ensembles of atoms occupying both states.

The ac Stark shift is proportional to the polarizability at finite frequency. The finite frequency dipole polarizability for state i is written

$$\alpha_i(\omega) = \sum_n \frac{f_{in}^{(1)}}{\epsilon_{in}^2 - \omega^2}, \tag{8}$$

where ω is the energy of the photon of the ac field.

The calculation of the $2s^2\ ^1S^e$ frequency-dependent polarizability uses Eq. (8) in much the same way as the static dipole polarizability is determined. The photon energy is included in the energy denominator when summing the oscillator strengths. The two electron energies of all states listed in Table I have been set to the experimental values for this calculation.

Figure 1 shows the frequency-dependent polarizabilities of the $2s^2\ ^1S^e$ ground states and the $2s2p\ ^3P_0^o$ levels as a function of photon energy. The $2s2p\ ^3P_0^o$ α_d and $S(-4)$ are both larger than that of the ground state. This means the first magic wavelength does not occur until the photon energy is large enough to excite the $2s2p\ ^3P_0^o \rightarrow 2s3s\ ^3S_1^e$ excitation. The lowest-energy magic wavelength is 300.2 nm. The next magic wavelength occurs after the $2s2p\ ^3P_0^o \rightarrow 2p^2\ ^3P_1^e$ excitation and is 252.3 nm.

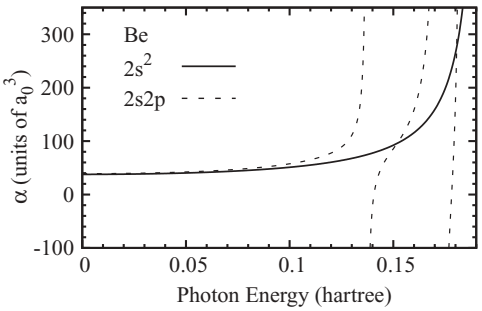

FIG. 1. The polarizability for the $2s^2$ ground state and the scalar polarizability of the $2s2p\ ^3P_0^o$ state as a function of photon energy (in hartree).

H. Some comments on accuracy

The primary results from the present work are the polarizabilities and magic wavelengths. To a large extent, the evaluation of these properties is dominated by a few key transitions. Since experimental energy differences were used in the polarizability and magic wavelength calculations, the primary contributions to the uncertainties are the $2s^2\ ^1S^e \rightarrow 2s2p\ ^1P^o$, $2s2p\ ^3P_0^o \rightarrow 2s3s\ ^3S^e$, $2s2p\ ^3P_0^o \rightarrow 2p^2\ ^3P_1^e$, and $2s2p\ ^3P_o^e \rightarrow 2s2p\ ^3P_1^o$ matrix elements.

The uncertainty in $|\langle 2s^2;{}^1S^e \parallel r\mathbf{C}^1(\hat{\mathbf{r}}) \parallel 2s2p;{}^1P^o\rangle|^2$ can be set to 0.5% [37]. All the key triplet oscillator strengths agree with the completely independent BCICP calculations to well within 0.5%; so ascribing an uncertainty of $\pm 1\%$ in these matrix elements can be regarded as conservative. Calculations of the polarizabilities and magic wavelengths were made by manually adjusting the matrix elements listed above and noting the outcomes.

The ground-state polarizability can be written as $37.73(18)a_0^3$. The scalar polarizability of the $^3P_0^o$ state can be written as $39.04(28)a_0^3$, while the tensor polarizability was $0.541(127)a_0^3$. The magic wavelengths are now 300.2(6) and 252.3(1) nm. The variation of the $^3P^o$ state α_d with frequency is so rapid that the magic wavelength is not that sensitive to small changes in the matrix elements.

The uncertainty in the $E1$ BBR shift can be written as

$$\delta(\Delta\nu_{\rm BBR}) = \Delta\nu_{\rm BBR}\left(\frac{\delta(\Delta\alpha_d)}{\Delta\alpha_d} + \frac{4\delta T}{T}\right), \tag{9}$$

with $\Delta\alpha_d = 1.31$ a.u., and setting $\delta T = 0$ gives $\Delta\nu_{\rm BBR} = -0.0112(32)$ Hz. The uncertainty in the $M1$ BBR shift is not likely to exceed 10% so an overall estimate of the total BBR shift would be $-0.018(4)$ Hz. The small value of $\Delta\nu_{\rm BBR}$ means uncertainties in the temperature of the BBR radiation field do not lead to a large uncertainty in the BBR shift.

IV. CONCLUSIONS

Large-scale CI calculations have been used to generate polarizabilities for the three lowest atomic states of neutral

beryllium. The underlying accuracy of the calculation was tested by comparing oscillator strengths involving low-lying states with other large-scale calculations [29,30]. The overall level of agreement was at the 1% level.

The most interesting feature of the present excited-state calculations is the very small difference between the polarizabilities of the $2s^2\ {}^1S^e$ state and the metastable $2s2p\ {}^3P_0^o$ state. This means an optical clock based on these two states will have an anomalously small BBR shift. The BBR shift is so small that consideration needs to be given to the second-order shift arising from the magnetic dipole component of the ambient electromagnetic field. The very small energy difference between the $2s2p\ {}^3P_0^o$ and ${}^3P_1^o$ state enhances the size of the BBR magnetic dipole shift and makes a significant contribution to the small BBR shift. The magnetic dipole BBR shift for the ${}^3P_2^o$ state is opposite in sense to the electric dipole component of the BBR shift.

The beryllium atom clock transition has the valuable feature that it has the smallest BBR of any group II or IIB atom [7]. Indeed, its BBR shift is one order of magnitude smaller than any of the neutral atoms proposed as a possible optical lattice clock. From the narrow point of view of giving paramount importance to reducing the size of the BBR shift, the beryllium atom represents the optimum choice to serve as a neutral atom-based optical frequency standard. However, there are other more pragmatic considerations that apply, such as actually devising a way to cool neutral beryllium, and right now the present results are best regarded as a potentially useful theoretical curiosity.

ACKNOWLEDGMENTS

The work of J.M. was supported in part by Australian Research Council Discovery Project DP-1092620.

[1] T. Binnewies, G. Wilpers, U. Sterr, F. Riehle, J. Helmcke, T. E. Mehlstäubler, E. M. Rasel, and W. Ertmer, Phys. Rev. Lett. **87**, 123002 (2001).
[2] G. Wilpers, T. Binnewies, C. Degenhardt, U. Sterr, J. Helmcke, and F. Riehle, Phys. Rev. Lett. **89**, 230801 (2002).
[3] J. Weiner, V. S. Bagnato, S. Zilio, and P. S. Julienne, Rev. Mod. Phys. **71**, 1 (1999).
[4] H. Katori, M. Takamoto, V. G. Pal'chikov, and V. D. Ovsiannikov, Phys. Rev. Lett. **91**, 173005 (2003).
[5] M. M. Boyd, A. D. Ludlow, S. Blatt, S. M. Foreman, T. Ido, T. Zelevinsky, and J. Ye, Phys. Rev. Lett. **98**, 083002 (2007).
[6] J. Ye, H. J. Kimble, and H. Katori, Science **320**, 1734 (2008).
[7] J. Mitroy, M. S. Safronova, and C. W. Clark, J. Phys. B **43**, 202001 (2010).
[8] S. G. Porsev and A. Derevianko, Phys. Rev. A **74**, 020502(R) (2006).
[9] J. Mitroy and M. W. J. Bromley, Phys. Rev. A **68**, 052714 (2003).
[10] J. Mitroy and M. W. J. Bromley, Phys. Rev. A **70**, 052503 (2004).
[11] W. Müller, J. Flesch, and W. Meyer, J. Chem. Phys. **80**, 3297 (1984).
[12] H.-J. Werner and W. Meyer, Phys. Rev. A **13**, 13 (1976).
[13] G. Diercksen, Chem. Phys. **65**, 407 (1982).
[14] D. Bégué, M. Mérawa, and C. Pouchan, Phys. Rev. A **57**, 2470 (1998).
[15] A. J. Thakkar, Phys. Rev. A **40**, 1130 (1989).
[16] D. Tunega, Chem. Phys. Lett. **269**, 435 (1997).
[17] J. Komasa, Phys. Rev. A **65**, 012506 (2001).
[18] S. G. Porsev and A. Derevianko, JETP **102**, 195 (2006).
[19] D. Begue, M. Merawa, M. Rerat, and C. Pouchan, J. Phys. B **31**, 5077 (1998).
[20] W. J. Stevens and F. P. Billingsley, Phys. Rev. A **8**, 2236 (1973).
[21] W. D. Robb, J. Phys. B **6**, 945 (1973).
[22] M. W. J. Bromley and J. Mitroy, Phys. Rev. A **65**, 062505 (2002).
[23] J. Mitroy, Aust. J. Phys. **52**, 973 (1999).
[24] L.-Y. Tang, J.-Y. Zhang, Z.-C. Yan, T.-Y. Shi, J. F. Babb, and J. Mitroy, Phys. Rev. A **80**, 042511 (2009).
[25] S. Hameed, A. Herzenberg, and M. G. James, J. Phys. B **1**, 822 (1968).
[26] S. Hameed, J. Phys. B **5**, 746 (1972).
[27] N. Vaeck, M. Godefroid, and C. Froese Fischer, Phys. Rev. A **46**, 3704 (1992).
[28] Y. Ralchenko, A. Kramida, J. Reader, and NIST ASD Team, NIST Atomic Spectra Database Version 3.1.5 (2008) [http://physics.nist.gov/asd3].
[29] C. Froese Fischer and G. Tachiev, At. Data Nucl. Data Tables **87**, 1 (2004).
[30] M. K. Chen, J. Phys. B **31**, 4523 (1998).
[31] I. Martinsen, A. Gaupp, and L. J. Curtis, J. Phys. B **7**, L463 (1974).
[32] R. E. Irving, M. Henderson, L. J. Curtis, I. Martinson, and P. Bengtsson, Can. J. Phys. **77**, 137 (1999).
[33] H. Kerkhoff, M. Schmidt, and P. Zimmermann, Phys. Lett. A **80**, 11 (1980).
[34] J. Bromander, Phys. Scr. **4**, 61 (1971).
[35] J. Y. Zhang and J. Mitroy, Phys. Rev. A **76**, 022705 (2007).
[36] Z. C. Yan, J. F. Babb, A. Dalgarno, and G. W. F. Drake, Phys. Rev. A **54**, 2824 (1996).
[37] J. Fleming, M. R. Godefroid, K. L. Bell, A. Hibbert, N. Vaeck, J. Olsen, P. Jönsson, and C. Froese Fischer, J. Phys. B **29**, 4347 (1996).
[38] W. M. Itano, L. L. Lewis, and D. J. Wineland, Phys. Rev. A **25**, 1233 (1982).
[39] J. Mitroy, J. Y. Zhang, M. W. J. Bromley, and K. G. Rollin, Eur. Phys. J. D **53**, 15 (2009).
[40] C. E. Moore, *Atomic Energy Levels (Molybdenum-Actinium NSRDS-NBS 35)* (US Government Printing Office, Washington DC, 1971), Vol. 3.
[41] A. Kramida and W. C. Martin, J. Phys. Chem. Ref. Data **26**, 1185 (1997).